

# High-frequency acousto-optic mode locker for picosecond pulse generation

U. Keller, K. D. Li, B. T. Khuri-Yakub, and D. M. Bloom

Ginzton Laboratory, Stanford University, Stanford, California 94305

K. J. Weingarten and D. C. Gerstenberger

Lightwave Electronics Corporation, 1161 San Antonio Road, Mountain View, California 94043

Received July 17, 1989; accepted October 27, 1989

We modeled, designed, and built a 500-MHz acousto-optic mode locker with a diffraction efficiency of 28% per 1 W drive power. The transducer is zinc oxide sputtered onto a sapphire substrate. A new figure of merit is defined for the mode-locker design, which indicates that sapphire is a good substrate material. Pulse widths of less than 10 psec with an average power of 150 mW were achieved from a 500-MHz pulse-rate, diode-pumped, cw mode-locked Nd:YLF laser using a pump power of 700 mW.

An increase in the pulse rate of mode-locked lasers improves performance in several ways. The mechanical stability of the laser increases, because the laser cavity is shorter, resulting in better operating stability and lower noise performance. In addition, both the pulse duration, which varies inversely as the square root of the laser repetition rate  $f_L$ , and the buildup time to reach the steady-state pulse duration, which varies inversely as the square of  $f_L$ , are reduced by increasing the laser repetition frequency.<sup>1</sup> This is especially important for generating short mode-locked laser pulses using solid-state laser materials such as Nd:YLF and Nd:glass, which have wider gain bandwidths  $\Delta f_a$  than Nd:YAG because the buildup time varies directly as  $\Delta f_a$ . Traditionally, fused quartz has been used as the substrate in mode lockers partially because of its excellent optical quality, which ensures low insertion loss in lasers. However, fused quartz is not suitable as a mode-locker material at higher repetition frequencies because it has a high acoustic attenuation that increases as the square of the rf drive frequency.<sup>2</sup> Therefore a new mode-locker substrate material with good optical qualities and low acoustic loss was needed. By modeling the mode locker with the Krimholtz-Leedom-Matthaei (KLM) model,<sup>3</sup> we determined a new figure of merit that shows that sapphire is an attractive substrate material. We have built and modeled a 500-MHz acousto-optic mode locker consisting of a zinc oxide (ZnO) transducer sputtered onto a sapphire substrate and have obtained a diffraction efficiency of 28% per 1 W of drive power. This mode locker was a key component in a diode-pumped mode-locked laser.<sup>4</sup> Recently, 9-psec pulses from a frequency-modulated mode-locked Nd:YLF laser have been reported,<sup>5</sup> for which, however, a Lorentzian pulse shape was assumed (i.e., 18-psec autocorrelation at FWHM). Pulses below 10 psec have been reported with mode-locked Nd:glass lasers.<sup>6,7</sup> However, stability<sup>7</sup> was a problem because stable pulses on

the sampling scope were never observed at the same time that the shortest pulses were measured with an autocorrelator.

The mode locker consists of an acousto-optic crystal substrate and a transducer that launches an acoustic wave into the substrate. The laser light is loss modulated at twice the rf drive frequency owing to the acoustic standing wave in the mode-locker substrate. The transducer can be treated as a three-port network, where two ports are defined by their acoustic impedances at each transducer interface  $Z_1$  and  $Z_2$  and the third port is defined by the electrical input impedance  $Z_3$ . The results are summarized by the KLM model.<sup>3</sup> In the case of a high- $Q$  acousto-optic mode locker, one acoustic port of the transducer is air backed (i.e.,  $Z_1 = 0$ ) and the other port is determined by the substrate that forms an acoustic resonator. The impedance transformation law<sup>8</sup> is used to calculate the acoustic impedance  $Z_2$ , which includes the substrate of thickness  $d$ , and the acoustic attenuation in the substrate, and the substrate-air interface ( $\approx 100\%$  reflector for acoustic waves). With the three-port equation,<sup>9</sup> the electrical input impedance  $Z_3$  of the mode locker and the acoustic force  $F_2$  at the transducer-substrate interface can then be determined. The known boundary conditions at the transducer-substrate interface ( $F_2$ ) and the substrate-air interface ( $F = 0$ ) determine the amplitudes of the two counterpropagating plane waves, which form the standing wave in the substrate. The known force amplitudes determine the refractive-index change in the substrate,<sup>10</sup> which then determines the diffraction efficiency [Eq. (2) below]. The frequency response of the transducer can be neglected with respect to the individual acoustic resonances. Assuming that all the losses are dominated by the acoustic attenuation  $\alpha$  in the substrate, it can be shown numerically that the refractive-index change is constant with frequency for a fixed absorbed power  $P_3$ , which is the difference between the incident and the

**Table 1. Acoustic Figure of Merit  $M$  and the New Figure of Merit  $M'$  for an rf Drive Frequency of 250 MHz and a Substrate Thickness of 5 mm<sup>a</sup>**

	Fused Quartz	Sapphire (Al <sub>2</sub> O <sub>3</sub> )	YAG (Y <sub>3</sub> Al <sub>5</sub> O <sub>12</sub> )	LiNbO <sub>3</sub>
$M$	$1.51 \times 10^{-15b}$	$0.22 \times 10^{-15c}$	$0.073 \times 10^{-15b}$	$6.99 \times 10^{-15b}$
$M'$	$2.82 \times 10^{-14}$	$2.82 \times 10^{-13}$	$4.3 \times 10^{-14}$	$4.66 \times 10^{-12}$

<sup>a</sup> Acoustic attenuation for all materials is given in Ref. 2.

<sup>b</sup> Ref. 3, Table B.7.

<sup>c</sup> Ref. 12.

reflected electrical power. This simplifies the final solution significantly because the frequency dependence of the refractive-index change is determined only by the absorbed power  $P_3(f)$ , which exhibits a strong resonance for a fixed available rf drive power and is determined by the electrical input impedance of the mode locker. The analytical solution for the refractive-index change with  $\alpha d \ll 1$  is then given by

$$\Delta n_0 \cong \frac{1}{\sqrt{2}} \left( \frac{M P_3}{\alpha d A} \right)^{1/2}, \quad (1)$$

where  $M$  is the acoustic figure of merit,<sup>11</sup>  $d$  is the substrate thickness, and  $A$  is the transducer area. Note that the solution given in relation (1) is an upper bound because of the assumption that the acoustic attenuation in the substrate is the dominant loss term in the mode locker. The diffraction efficiency  $\eta$  at the Bragg angle  $\theta_B$  of incidence is then given by<sup>3</sup>

$$\eta(t) = \sin^2(\theta_m \sin \omega t), \text{ with } \theta_m = \frac{\pi}{\lambda_0} \Delta n_0 L \cos \theta_B, \quad (2)$$

where  $\theta_m$  is the modulation index,  $\lambda_0$  is the vacuum light wavelength,  $\Delta n_0$  is determined by relation (1), and  $L$  is the transducer length.

From relation (1) it follows that the appropriate figure of merit for the mode-locker design is given by

$$M' = \frac{M}{\alpha d} \quad (3)$$

and not just by the acoustic figure of merit  $M$ . Especially at higher frequencies, the acoustic attenuation becomes the dominant parameter, increasing as the square of the frequency.<sup>2</sup> For example, at 250 MHz and  $d = 5$  mm,  $M = 0.22 \times 10^{-15}$  (Ref. 12) and  $M' = 2.8 \times 10^{-13}$  [Eq. (3) and Ref. 2] for sapphire in SI units, whereas for fused quartz  $M = 1.51 \times 10^{-15}$  (Ref. 3) and  $M' = 2.8 \times 10^{-13}$  [Eq. (3) and Ref. 2], 10 times less than for sapphire (see Table 1). We did not consider semiconductors, which typically have large acoustic figures of merit, because of deep-level absorption for infrared wavelengths.<sup>13</sup> LiNbO<sub>3</sub> was not chosen because of possible optical damage within the laser cavity.

We chose optical-quality sapphire as the substrate material with a thickness of 5 mm to provide a suitably large clear aperture for the optical beam. The crystal  $c$  axis is perpendicular to the transducer interface, giving longitudinal acoustic waves that have much lower acoustic losses than shear waves do. The substrate interfaces for the optical beam are slightly wedged to minimize étalon effects inside the cavity. The acoustic interfaces are polished plane parallel to

better than a few optical fringes, which becomes more critical the higher the drive frequency. The mode locker was also designed to be as compact as possible to permit close positioning to the end mirror and to reach thermal equilibrium quickly.

The ZnO transducer is fabricated as follows. Titanium (5.0–10.0 nm thick) is deposited onto the substrate first to serve as a sticking layer. A (111)-oriented gold film (150.0 nm thick) is deposited onto one side of the substrate, covering approximately two thirds of the surface. ZnO is then sputtered to the desired thickness. The best transducer thickness as predicted by the KLM model is approximately a half-wavelength when the characteristic impedance of the substrate is smaller than that of the transducer material and approximately a quarter-wavelength thick in the other case. For a quarter-wavelength 250-MHz transducer, 6.3  $\mu$ m of ZnO was grown. The top gold electrode (150.0 nm thick) is then deposited. The area where the two electrodes overlap determines the transducer area, which is in this case 0.9 mm  $\times$  3 mm. The top electrode has a finger hanging out to the side that does not overlap the lower electrode to permit wire bonding on an area away from the ZnO and to avoid possible damage to the transducer.

After the transducer fabrication the optical interfaces of the mode locker are antireflection coated. The mode locker finally is mounted into a compact high-frequency package shown in Fig. 1. The mode locker is attached with silver epoxy to the gold-plated brass holder that acts as a heat sink and the ground contact for the lower transducer electrode.

The measured diffraction efficiency for 1.06- $\mu$ m-wavelength light as a function of absorbed drive power for a 500-MHz mode locker agrees well with our model

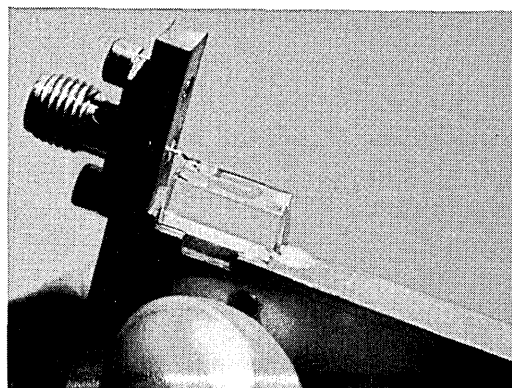


Fig. 1. ZnO-sapphire mode locker mounted in a high-frequency package.

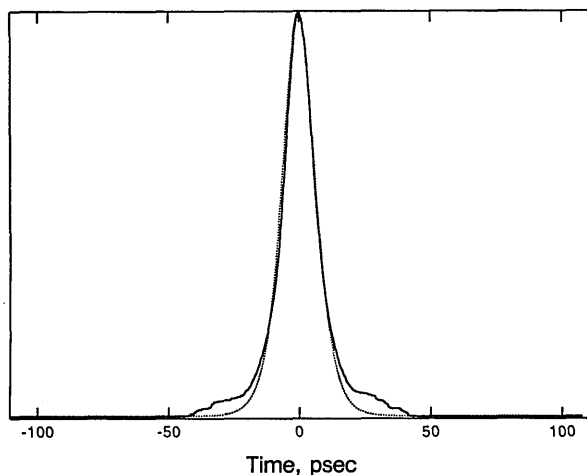


Fig. 2. Autocorrelation traces: averaged 16 times (solid curve) and a  $\text{sech}^2$  autocorrelation fit (dotted curve).

given by relations (1) and (2).<sup>4</sup> A diffraction efficiency of 28% per 1 W absorbed power was measured with a reflection loss (or return loss) of less than 10% (-10 dB). A 500-MHz ZnO-fused quartz mode locker with a 3-mm substrate thickness was also fabricated, and its performance, a diffraction efficiency of 5.6% per 1 W, was also well predicted by the KLM model. Longer transducer lengths will give higher diffraction efficiencies [Eq. (2)]. For example, with a transducer length of 5 mm and a substrate thickness of 4 mm, the KLM model predicts that a 2-GHz ZnO-sapphire mode locker (i.e., a 1-GHz rf drive frequency) still gives 10% per 1 W diffraction efficiency.

We used the mode locker in a diode-pumped, cw mode-locked Nd:YLF laser. The cavity was a linear folded-cavity design,<sup>5</sup> where an angle of 17° corrects for the astigmatism from the turning mirror with a 150-mm radius of curvature.<sup>14</sup> The cavity was end pumped with two 500-mW diode-laser arrays from Spectra Diode (Model 2432). A 5-mm Nd:YLF rod had its flat end high-reflection coated for the laser wavelength and antireflection coated for the diode-laser pump, and the other end was cut at Brewster's angle. The output coupler is a flat mirror with 5% transmission and was additionally wedged at 10' in order to minimize unwanted étalon effects in the cavity. The nominal Nd<sup>3+</sup> concentration was 1%. With a pump power of 700 mW at the crystal and an insertion loss of the mode locker of 2-3%, we achieved an average output power of approximately 150 mW at 1.047 μm with a pulse duration of approximately 9 psec FWHM. We are assuming that the pulse is time-bandwidth limited, justified by prior experience with amplitude-modulated mode-locked lasers. A typical

autocorrelation (Fig. 2), averaged over many scans, compares well with an ideal 9.1-psec FWHM hyperbolic-secant-squared autocorrelation (i.e., 14-psec autocorrelation FWHM), except for some small shoulders on the pulse. We speculate that the shoulders are due to some étalon effects between the mode locker and the output coupler. The pulses were relatively stable and reproducible but sensitive to small changes in the cavity length, such as from tweaking mirror alignment or changes to the mode-locker drive frequency of tens of hertz.

In conclusion, we have built a 500-MHz ZnO-sapphire acousto-optic mode locker with which a diffraction efficiency of 28% per 1 W was achieved. A new figure of merit was defined and used as a design guideline for the mode-locker substrate. This mode locker was a key component in a diode-pumped cw mode-locked Nd:YLF laser that gives pulse widths of less than 10 psec with 150 mW of average output power, suitable for applications such as optical probing of integrated circuits, testing of high-speed optoelectronic components, and as sources for laser-driven particle accelerators.

This research was partially supported by U.S. Air Force Office of Scientific Research contract F49620-88-C-0103 and U.S. Department of Energy Small Business Innovative Research contract DE-AC03-88ER80653.

## References

1. D. J. Kuizenga and A. E. Siegman, *IEEE J. Quantum Electron.* **QE-6**, 694 (1970).
2. B. A. Auld, *Acoustic Fields and Waves in Solids* (Wiley, New York, 1973), Vol. 1, Fig. 3.11.
3. G. S. Kino, *Acoustic Waves: Devices, Imaging and Analog Signal Processing* (Prentice-Hall, Englewood Cliffs, N.J., 1987).
4. U. Keller, K. J. Weingarten, K. D. Li, D. C. Gerstenberger, P. T. Khuri-Yakub, and D. M. Bloom, in *Digest of Conference on Lasers and Electro-Optics* (Optical Society of America, Washington, D.C., 1989), paper PD2.
5. G. T. Maker and A. I. Ferguson, *Electron. Lett.* **25**, 1025 (1989).
6. L. Yan, J. Ling, P.-T. Ho, and C. Lee, *Opt. Lett.* **11**, 502 (1986).
7. S. Basu and R. L. Byer, *Opt. Lett.* **13**, 458 (1988).
8. R. E. Collin, *Foundations for Microwave Engineering* (McGraw-Hill, New York, 1966), p. 317.
9. Ref. 3, p. 32.
10. Ref. 3, p. 504.
11. Ref. 3, p. 506.
12. *J. Res. Natl. Bur. Stand. Sect. A* **74**, 215 (1970).
13. G. M. Martin, *Appl. Phys. Lett.* **39**, 747 (1981).
14. D. C. Hanna, *IEEE J. Quantum Electron.* **QE-5**, 483 (1969).